28. Y. Yasui, K. Itoh, H. Kamiya, T. Ino, N. Mizuno, *J. Comp. Neurol.* **274**, 91 (1988).
29. J. R. Dostrovsky, R. R. Tasker, S. E. B. Wells, L. Lee, paper presented at the Symposium on Neurobiology of Nociception, Kawai, HI, 9 to 12 April 1990.
30. M. C. Bushnell and G. H. Duncan, *Exp. Brain Res.*, in (*17*).
31. S. Y. Musil and C. R. Olson, *J. Comp. Neurol.* **272**, 203 (1988).
32. PET data from a no-stimulation "Baseline" condition were collected for six subjects (in addition to data from the Heat Pain and Warm conditions). Subtractive analysis of Warm minus Baseline revealed no tendency ($t = -0.70$) toward activation at or near the prominent anterior cingulate focus observed with the Heat Pain condition.
33. R. Melzack and K. L. Casey, *The Skin Senses*, D. R. Kenshalo, Sr., Ed. (Thomas, Springfield, IL, 1968), pp. 423–443.
34. M. A. Mintun, P. T. Fox, M. E. Raichle, *J. Cereb. Blood Flow Metab.* **9**, 96 (1989).
35. P. T. Fox *et al.*, *ibid.* **8**, 642 (1988).
36. We thank the staff of the McConnell Brain Imaging Centre, the Medical Cyclotron Unit, and the Neurophotography Department for their technical assistance, and A. Gjedde and J. Lund for comments on the manuscript. Special thanks to P. Neelin, L. Collins, G. Filosi, and G. Lambert for technical assistance. Supported by Canadian Medical Research Council, the Isaac Walton Killam Fellowship Fund of the Montreal Neurological Institute, and the McDonnell-Pew Foundation.

5 October 1990; accepted 4 January 1991

Movement of Neural Activity on the Superior Colliculus Motor Map During Gaze Shifts

DOUGLAS P. MUNOZ,* DENIS PÉLISSON,† DANIEL GUITTON‡

The superior colliculus contains neurons that cause displacements of the visual axis (gaze shifts). These cells are arranged topographically in a motor map on which the vector (amplitude and direction) of the coded movement varies continuously with location. How this spatial representation becomes a temporal code (frequency and duration) in the motoneurons is unknown. During a gaze shift, a zone of neural activity moved continuously on the map from an initial location, defining the vector of the desired gaze shift, to a final "zero" position containing neurons that were active during fixation. Thus, the spatial-temporal transformation may be accomplished by control of gaze throughout the spatial trajectory of activity on the motor map.

THE MAMMALIAN SUPERIOR COLLICULUS (SC) is a laminated neural structure that transforms sensory information into motor commands that rapidly move the visual axis (*1*). Visually responsive neurons in the superficial layers are organized into a retinotopic map of visual space, subtending up to 80° of the contralateral visual field (*2*). Here we investigated the deeper layers, which are organized into a motor map (*1*).

In the cat, the animal studied here, coordinated eye-head movements are used to look at targets situated farther than about ±10° from center (*3*). Microstimulation of the deeper layers, in the cat whose head is unrestrained, elicits topographically coded gaze (gaze = eye-in-space = eye-in-head + head-in-space) shifts in which the vectors are predicted by the location being stimulated on the motor map (*4*). This motor map is retinotopically coded and is in spatial register with the overlying visual map.

The deeper layers contain tectoreticular neurons (TRNs) that control gaze shifts via projections to contralateral brainstem regions that generate eye and head movements (*5*). TRNs have both multimodal sensory responses (*6*) and movement-related discharges (*7–9*). Many TRNs burst just before a gaze shift. These neurons are grouped on the motor map into a large, nearly circular zone, the center of which specifies the amplitude and direction of the intended gaze shift. Other TRNs, located in the zero-amplitude location at the rostral pole of the SC, are active when the cat fixates a target and are silent during orienting gaze shifts (*8, 10*). Therefore, the retinotopic position of the ensemble of active TRNs differs if measured at the start and end of a gaze shift. In our experiments, we determined, in the cat, the retinotopic location of the active ensemble of neurons during a gaze shift (*11*).

We analyzed the activity of TRNs identified on the basis of their antidromic response after stimulation of the contralateral predorsal bundle (*7, 8*). The animal was required to make predictive gaze shifts to a spatial locus devoid of a newly appearing sensory cue, a procedure that prevented phasic visual responses from contaminating the movement-related neuronal activity.

The movement-related discharges of two TRNs, cells Q24 and Q37, recorded in the same cat are shown in Fig. 1. Of the two

Montreal Neurological Institute, Department of Neurology and Neurosurgery, McGill University, 3801 University, Montréal, Québec, Canada H3A 2B4.

*Present address: Laboratory of Sensorimotor Research, National Eye Institute, National Institutes of Health, Building 10, Room 10c101, Bethesda, MD 20892.
†Present address: Vision et Motricité, INSERM, U-94, 16 avenue du Doyen Lepine, 69500 Bron, France.
‡To whom correspondence should be addressed.

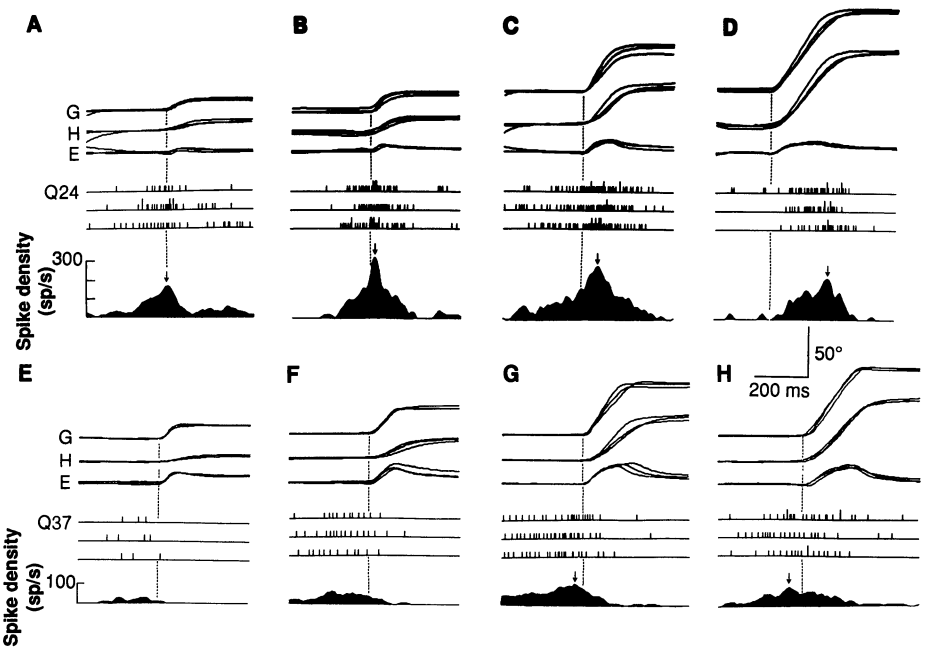

Fig. 1. Movement-related discharges of TRNs. Shown in each panel are the gaze (G), head (H), and eye (E) position traces; neural discharge for cells Q24 (**A** to **D**) and Q37 (**E** to **H**); and spike density function [number of action potentials (spikes) per second (sp/s)] (*11*). The occurrence of an action potential is represented by a small vertical line. Additional small lines superimposed on top of others indicate extra spikes within the same 2-ms time bin. The preferred movements for cell Q24 were directed horizontally and for cell Q37 were directed down to the left at an angle of about 45° to the horizontal. Traces are aligned on gaze-shift onset (vertical dashed lines). Arrows, maximum spike density.

cells, Q24 was located more rostrally (*12*). This cell discharged in relation to all predictive gaze shifts, made in the cell's preferred direction, that were larger than about 5° in amplitude. The timing of the discharge depended on the amplitude of movement: as gaze shift amplitude increased (10°, 17°, 40°, 80° in Fig. 1, A to D, respectively) the peak discharge occurred progressively farther from the start of the gaze shift. Indeed, for 80° gaze shifts (Fig. 1D), the cell was silent at movement onset.

Cell Q37 was most active before the 50° and 70° gaze shifts (Fig. 1, G and H), had a weak discharge before the 25° movement (Fig. 1F), and gave only a few spikes before the 10° movement (Fig. 1E) (*13*).

For each cell, we plotted the latency to the peak of the burst discharge from onset (Fig. 2A) or termination (Fig. 2B) of each gaze shift as a function of the total amplitude of the gaze displacement. Only movements that consisted of a single-step gaze shift along the cell's preferred direction were considered (Fig. 1). As total gaze displacement increased, the latency from the end of each gaze shift to peak discharge remained constant for cell Q24 (Fig. 2B). Hence the discharge of Q24 was greatest near a fixed position of gaze relative to the target. It follows that the latency from movement onset to peak discharge for Q24 increased with the amplitude of the gaze displacement (Fig. 2A) because the duration of gaze shifts normally increases with amplitude (*3*). By comparison, Q37 reached peak discharge at constant latency before gaze shifts in the amplitude range 30° to 80° (Fig. 2A) and therefore at decreasing (that is, increasingly negative) latencies relative to the end of gaze shifts in that range (Fig. 2B). Q37 was virtually silent for gaze shifts smaller than about 30°. The nine TRNs that we studied in detail were clustered, functionally, into two groups: cells 1 to 5 (including Q24) were recorded in the anterior SC (amplitudes less than 30° on the motor map); cells 6 to 9 (including Q37) were recorded in the more caudal SC (amplitudes greater than 50°) (Fig. 2, D and E).

We also compared the instantaneous firing frequency of each cell [using the average spike density function (*11, 14*)] to the corresponding value of instantaneous gaze error (difference between final and current gaze positions) for different amplitude gaze shifts (Fig. 2, C and F). For each cell, the curves corresponding to different gaze shifts tended to join a common trajectory, regardless of the total gaze displacement. The peak discharge for different amplitudes of movement was similar and was attained at a specific value of instantaneous gaze error: between 8° and 12° for cell Q24 and between 50° and 70° for cell Q37. Comparable plots of spike density as a function of either instantaneous eye or head error revealed no (for the eye) or weaker (for the head) overlaps for different amplitude movements (*15*).

The data in Figs. 1 and 2 are inconsistent with the classic notion that vector-tuned neurons in the SC specify initial motor error (*1, 16*). Rather, our results indicate that a zone of TRN activity moves across the SC of the cat during the course of an orienting gaze shift (*17*) (Fig. 2G). Immediately before a gaze shift, a zone of TRN activity is established in the caudal region of one SC at a location on the motor map that codes the initial vector error (say, 60° horizontal) that exists between the initial position of the visual axis and the target of interest. As the gaze shift proceeds, this zone of TRN activity moves toward the rostral pole. Its instantaneous location on the motor map specifies the remaining gaze error. As the gaze shift terminates (that is, gaze error is zero), the active zone invades the rostral pole, where fixation-related TRNs are located (*8, 10*). Discharges similar to those of cells Q37 and Q24 would be recorded by two microelec-

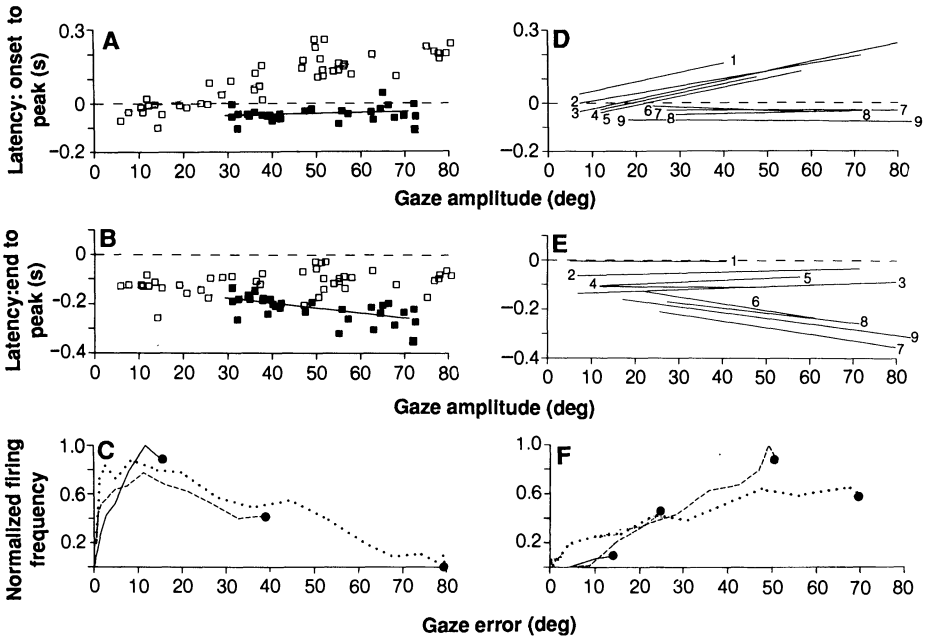

Fig. 2. (**A** and **B**) Latency from onset (A) and end (B) of a gaze shift to peak discharge for cells Q24 (□) and Q37 (■) as a function of the amplitude of gaze displacement. Each square represents data from one gaze shift. Negative values represent trials in which peak discharge preceded movement onset (A) and termination (B). Linear regression analysis correlation coefficient: (A) Q24, $r = 0.90$; (B) Q37, $r = -0.64$. (**D** and **E**) Linear regression lines for nine TRNs in which sufficient data were obtained. Correlation coefficients for lines 1 to 9, respectively, in (D): $r = 0.86, 0.90, 0.88, 0.65, 0.75, -0.25, -0.02, 0.20$, and -0.08; in (E): $r = -0.01, 0.42, 0.33, -0.01, 0.28, -0.66, -0.61, -0.64$, and -0.70. (**C** and **F**) Plots of Q24's (C) and Q37's (F) normalized instantaneous firing frequency as a function of instantaneous gaze error for different amplitude movements along the optimal direction. Each curve was obtained by (i) aligning three to seven gaze shifts of identical magnitude on the end of the gaze saccade and obtaining the average trajectory; (ii) calculating the corresponding average spike density function (*11*), which we then normalized using the highest of the peak values obtained in all of the trials that covered the whole amplitude range; and (iii) shifting the normalized average spike density function 8 ms to the right, a time that corresponds to the minimal delay between a sudden burst of activity in the tectoreticulospinal pathway and a midflight reacceleration of gaze (*8*). Time is implicit on each curve: it starts at the black circle, the start of a gaze shift, and progresses from right to left (that is, toward 0° gaze error). Measurement of firing frequency began at the onset of gaze shifts. (**G**) Proposed activity patterns in the TRN layer of the SC during the execution of an orienting gaze shift. Neural activity (firing frequency) is represented schematically as a hill protuding from the two-dimensional, oval surface of the SC motor map. The "zero" of the map is at the intersection, in the rostral pole, of the horizontal and vertical meridians. Each section shows the TRN layer at a different time. The black dots represent hypothetical recording sites that would yield data similar to that observed in Q37 and Q24, respectively. No scale intended.

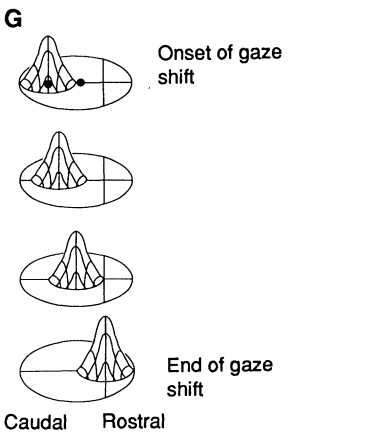

trodes located at the left and right black dots, respectively, on the top portion of Fig. 2G.

An alternative interpretation of the data is that a circular wave of activity propagates radially from an origin at the initial site of activation. Our data are not compatible with this notion. There was a lack of burst activity in TRNs located farther from the fixation zone than the initially active zone. For example, cell Q37 did not burst (Fig. 1E) after the start of 10° to 15° gaze shifts that began at the SC site of Q24.

Our observations suggest that a topographically represented motor command is transformed into the temporal firing pattern that motoneurons send to muscles (the so-called spatial temporal transform) when gaze is controlled throughout the spatial trajectory of neural activity on the motor map (*18*). This conclusion implies that traditional models of collicular control of gaze shifts need to be revised. In these models, the SC provides a command specifying only the initial vector of the intended gaze shift (*1*): a brainstem feedback control system is hypothesized to subtract actual gaze position from this signal, thereby yielding instantaneous gaze error, which drives the movement (*19*). Our results show that the SC itself spatially encodes the gaze error. Therefore, the SC may reside within the gaze feedback loop (*3, 8, 14*). This hypothesis is supported by observations that a sudden increase in the discharge frequency of TRN phasic bursts speeds up a gaze shift without affecting its accuracy (*8*). Such a finding is difficult to incorporate in traditional models of the SC, but, in a feedback control system wherein the SC provides the error signal, the higher velocities reduce gaze error more quickly, allowing shorter movement duration while maintaining accuracy.

REFERENCES AND NOTES

1. D. Guitton, in *Eye Movements*, R. H. S. Carpenter, Ed. (Macmillan, London, in press); D. L. Sparks, *Physiol. Rev.* **66**, 118 (1986); _____ and L. E. Mays, *Annu. Rev. Neurosci.* **13**, 309 (1990); R. H. Wurtz and J. E. Albano, *ibid.* **3**, 189 (1980).
2. A neuron in the superficial layers responds to visual stimuli restricted to a particular location in the contralateral half of the visual field. Neurons are arranged topographically to form a continuous representation (map) of this half-field (*1*).
3. D. Guitton, D. P. Munoz, H. L. Galiana, *J. Neurophysiol.* **64**, 509 (1990).
4. M. Crommelinck, M. Paré, D. Guitton, *Soc. Neurosci. Abstr.* **16**, 1082 (1990); D. Guitton, M. Crommelinck, A. Roucoux, *Exp. Brain Res.* **39**, 63 (1980); A. Roucoux, D. Guitton, M. Crommelinck, *ibid.*, p. 75.
5. A. Grantyn and R. Grantyn, *Exp. Brain Res.* **46**, 243 (1982); A. K. Moschovakis and A. B. Karabelas, *J. Comp. Neurol.* **239**, 276 (1985).
6. M. A. Meredith and B. E. Stein, *J. Neurophysiol.* **56**, 640 (1986).
7. D. P. Munoz and D. Guitton, *Brain Res.* **398**, 185 (1986).
8. D. P. Munoz, thesis, McGill University, Montreal (1988); _____ and D. Guitton, *Rev. Neurol. (Paris)* **145**, 567 (1989).
9. A. Berthoz, A. Grantyn, J. Droulez, *Neurosci. Lett.* **72**, 289 (1986); A. Grantyn and A. Berthoz, *Exp. Brain Res.* **57**, 417 (1985).
10. D. P. Munoz and D. Guitton, *Soc. Neurosci. Abstr.* **14**, 956 (1988); D. P. Munoz, D. M. Waitzman, R. H. Wurtz, *ibid.* **16**, 1084 (1990).
11. In six alert cats we studied the movement-related discharge characteristics of 16 antidromically identified TRNs. Of these, nine TRNs were recorded over a wide range of gaze-shift amplitudes, which provided the present database, whereas the other seven provided limited, but confirmatory, data. Methods have been described (*3, 8*). Cats were trained to generate orienting movements of different amplitudes and directions. An opaque barrier of variable width and orientation was positioned in front of the animal and a food target was presented on one side, then moved behind the barrier to remain hidden there. The trained animal oriented to the opposite side where it anticipated target reappearance. Thus, the animal oriented to a spatial locus devoid of a new sensory cue. Some experiments were designed [P. Pélisson, D. Guitton, D. P. Munoz, *Exp. Brain Res.* **78**, 654 (1989)] such that the animals oriented to the opposite side of the barrier in complete darkness. Similar results were obtained. To evaluate a neural discharge, it is usual to sum many responses into histograms, which give an estimate of the probability of an action potential occurring in each bin. To provide this estimate for single trials, we substituted Gaussian distributions, 20 ms wide, for each spike, thereby creating a spike probability density function (*14*). With this technique, the time of occurrence of a peak discharge was rarely ambiguous, but, when it was, the time of the earliest peak was plotted. The sum of such transformed rasters is the average spike density function.
12. More anterior positions on the motor map code smaller gaze shifts. The stereotactic position of Q24 was about 1.5 mm anterior to that of Q37. Microstimulation at the sites of Q24 and Q37 elicited 13° and 70° gaze shifts, respectively, which are close to the values predicted from Fig. 2.
13. The large range of gaze-shift amplitudes, over which the discharge of Q37 preceded movement onset, is characteristic of cells in the caudal SC and is due to the nonlinear characteristics of the motor map. In the caudal SC, a small zone of the motor map codes a wide range of amplitudes. Cell Q37 initiated ~60° gaze shifts. Extending the properties of cell Q24 to Q37 implies that the latter should discharge after the onset of gaze shifts larger than 60°. Given the compressed scaling of the posterior SC, 100° gaze shifts would probably have to be studied to discern this effect. Unfortunately, we could not test Q37 for amplitudes greater than 70° because our cats rarely generated such large single-step gaze shifts.
14. D. M. Waitzman, T. P. Ma, L. M. Optican, R. H. Wurtz, *ibid.* **72**, 649 (1988).
15. D. P. Munoz, D. Pélisson, D. Guitton, unpublished data.
16. In monkey, neurons that burst before saccades have finite movement fields: upper and lower limits in the direction and amplitude ranges over which the cell is active. By comparison, cat TRNs, such as cell Q24, had a lower limit on amplitude but no upper limit: they discharged for all amplitudes above the lower limit.
17. The limited range of eye motion (±25°) (*1, 3, 4*) in the cat prevented us from ascertaining whether or not these mechanisms operate to drive saccades in the cat whose head is held fixed.
18. Theoretical considerations related to and predicting moving activity patterns on the motor map of the SC were proposed by W. Pitts and W. S. McCullough [*Bull. Math. Biophys.* **9**, 127 (1947)]. Additional analyses have been conducted by J. Droulez and A. Berthoz [in *Neural Computers*, R. Eckmiller and C. v. d. Malsburg, Eds. (Springer-Verlag, Berlin, 1988), pp. 345–358; *Proc. Natl. Acad. Sci. U.S.A.*, in press], and P. Lefebvre and H. L. Galiana [*Soc. Neurosci. Abstr.* **16**, 1084 (1990)].
19. J. H. Fuller, H. Maldonado, J. Schlag, *Brain Res.* **271**, 241 (1983); D. Guitton, R. M. Douglas, M. Volle, *J. Neurophysiol.* **52**, 1030 (1984); D. Guitton and M. Volle, *ibid.* **58**, 427 (1987); V. P. Laurutis and D. A. Robinson, *J. Physiol. (London)* **373**, 209 (1986); D. Pélisson and C. Prablanc, *Brain Res.* **380**, 397 (1986); _____, C. Urquizar, *J. Neurophysiol.* **59**, 997 (1988); R. D. Tomlinson and P. S. Bahra, *ibid.* **56**, 1558 (1986).

20. Supported by the Medical Research Council of Canada, the Fonds de la Recherche en Santé du Québec, and a stipend from the Montreal Neurological Institute (D.P.M.).

10 August 1990; accepted 7 December 1990

Second Structural Motif for Recognition of DNA by Oligonucleotide-Directed Triple-Helix Formation

PETER A. BEAL AND PETER B. DERVAN*

Relative orientations of the DNA strands within a purine·purine·pyrimidine triple helix have been determined by affinity cleaving. A purine-rich oligonucleotide bound in the major groove of double-helical DNA antiparallel to the Watson-Crick purine strand. Binding depended upon the concentration of multivalent cations such as spermine or Mg^{2+}, and appeared to be relatively independent of pH. Two models with specific hydrogen-bonding patterns for base triplets (G·GC, A·AT, and T·AT) are proposed to explain the sequence specificity of binding. The two models differ in the conformation about the glycosyl bond (syn or anti) and the location of the phosphate-deoxyribose backbone in the major groove of DNA. This motif broadens the structural frameworks available as a basis for the design of sequence-specific DNA binding molecules.

PYRIMIDINE OLIGONUCLEOTIDES BIND specifically to purine sequences in double-helical DNA to form a local triple-helical structure (*1–4*). These oligonucleotides bind in the major groove parallel to the Watson-Crick (W-C) purine strand through the formation of Hoogsteen hydrogen bonds. Specificity is derived from thymine (T) recognition of adenine-thymine base pairs (T·AT base triplets) and protonated cytosine (C+) recognition of guanine-cytosine base pairs (C+GC) base triplets). Less well under-